Journal of Catalysis 261 (2009) 75–87

Contents lists available at ScienceDirect

Journal of Catalysis

www.elsevier.com/locate/jcat

Amino-based metal-organic frameworks as stable, highly active basic catalysts

Jorge Gascon *, Ugur Aktay, Maria D. Hernandez-Alonso, Gerard P.M. van Klink, Freek Kapteijn

Catalysis Engineering, DelftChemTech, Delft University of Technology, Julianalaan 136, 2628 BL Delft, The Netherlands

ARTICLE INFO

Article history:
Received 18 October 2008
Revised 4 November 2008
Accepted 4 November 2008
Available online 28 November 2008

Keywords:
IRMOF-3
MIL-53
MOF
Metal-organic frameworks
Knoevenagel condensation
Base-catalyzed reactions
Functional organic sites
Heterogeneous catalysis

ABSTRACT

Metal-organic frameworks (MOFs) with non-coordinated amino groups, i.e. IRMOF-3 and amino-functionalized MIL-53, are stable solid basic catalysts in the Knoevenagel condensation of ethyl cyanoacetate and ethyl acetoacetate with benzaldehyde. IRMOF-3_{DEF} exhibits activities that are at least as high as the most active solid basic catalysts reported, with a 100% selectivity to the condensation product. For IRMOF-3 samples the catalytic activity correlated with the accessibility of the basic sites. Diffusion limitations could be excluded for this most active catalyst. A new MOF based on the MIL-53 topology and non-coordinated amino groups has been synthesized and characterized. Although active its poor performance in the studied Knoevenagel condensations is attributed to strong adsorption and diffusion limitations in the 1-D pore structure of this framework. The performance of the IRMOF-3 catalysts demonstrates that the basicity of the aniline-like amino group is enhanced when incorporated inside the MOF structure, increasing the pK_a of the basic catalyst and more active than aniline as homogeneous catalyst. The IRMOF-3 catalysts are stable under the studied reaction conditions, and could be reused without significant loss in activity. The catalytic performance of IRMOF-3 in various solvents suggests that this open, accessible and well-defined structure behaves more like homogeneous basic catalysts, in contrast to other solid basic catalysts. By means of DRIFTS, the reaction mechanism has been elucidated, showing spectroscopic evidence of benzaldimine intermediates.

1. Introduction

The development of heterogeneous basic catalysts is a crucial requirement for sustainable chemistry [1]. Using solid catalysts, instead of stoichiometric amounts of soluble strong bases, the overall atom efficiency of reactions is improved, processes are simplified, the turn-over-number of the catalyst is increased, the volume of waste is significantly reduced, and product work-up becomes easier, if necessary at all. Compared to the broad application of solid acid catalysts, considerable less attention has been given to the development of solid basic catalysts [2]. Typically organic bases immobilized on different supports have been used as catalytic materials [3]. Progress has predominately been limited because of leaching of the active material from the various types of support used [3,4]. Other solid bases, such as layered double hydroxides or ion exchanged zeolites, are either very active when fresh but suffer from severe and rapid deactivation [5], or their initial activity is rather low [6].

Metal-organic frameworks (MOFs) constitute a new class of structured microporous materials, coordination polymers built up from organic linkers and inorganic connectors [7]. In principle, these MOFs can contain any functional group, especially connected to the organic linker, and the accessibility of these groups can be tailored to the application, from almost blocked to fully accessible. Although these properties make MOFs a promising class of new heterogeneous catalysts, it is generally acknowledged that the full potential of this new class of materials has not been identified [8]. Detailed studies on the catalytic performance of MOFs with catalysis taking place at the metal center have recently been published [9,10]. However, only a few proofs of concept of MOFs with catalytically-active functional organic sites (FOS, i.e. catalysis takes place at the organic linker [11]) have been reported [11–14]. Concerning base-catalyzed reactions, only Seo et al. [14] and Hasegawa et al. [11] have demonstrated the possibility to use as-synthesized MOFs as basic catalysts by introducing pyridyl and amide groups, respectively, in the organic linkers. However, the weak basicity of these functional groups implied only very low activities, while other important aspects such as recyclability and catalyst stability were not studied in further detail. Another approach to use MOFs as basic catalysts has been proposed very recently: the grafting of amino groups on coordinatively unsaturated metal centers of MOFs, yielding active catalysts for the Knoevenagel condensation of benzaldehyde with ethyl cyanoacetate [15]. However, deactivation of the catalyst due to leaching of the active sites seems to be an issue using this approach.

* Corresponding author.
E-mail address: j.gascon@tudelft.nl (J. Gascon).

0021-9517/$ – see front matter
doi:10.1016/j.jcat.2008.11.010

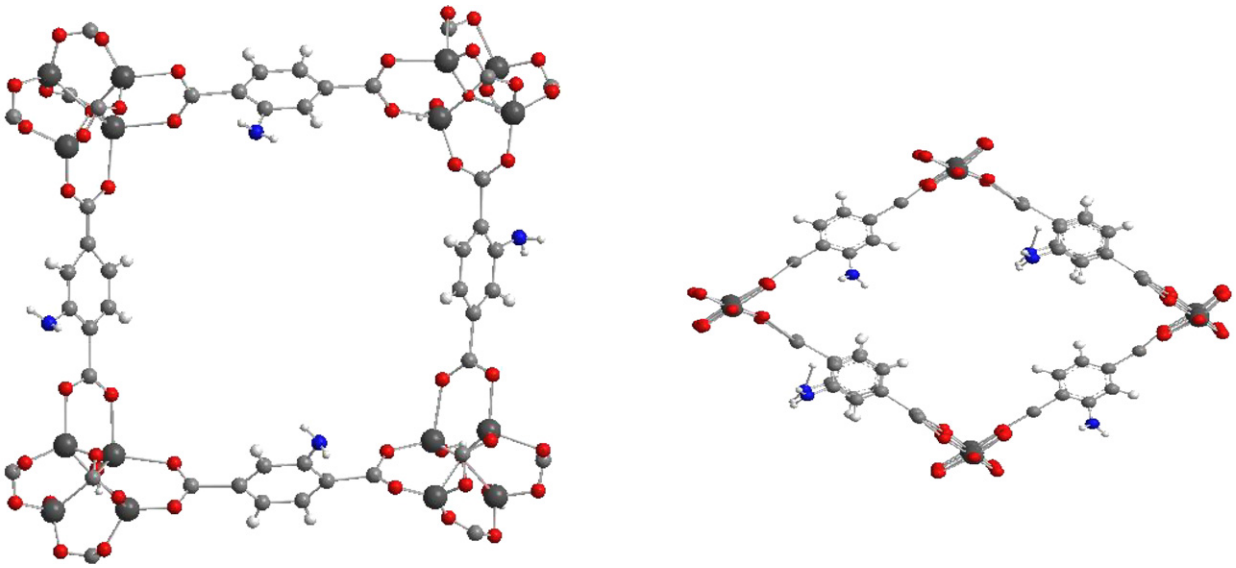

Fig. 1. Structure of the synthesized MOFs: (left) IRMOF-3, (right) amino-MIL-53(Al). (Oxygen atoms in red, carbon atoms in light gray, nitrogen atoms in blue, and Zn (left) and Al (right) in dark gray. For interpretation of the references to color in this figure legend, the reader is referred to the web version of this article.)

Although the synthesis and some applications of MOFs with amino groups have already been described [12,16], their use as basic catalysts has not yet been reported in the open literature. The best known amino-MOF is IRMOF-3, a member of the isoreticular MOF family first reported by Yaghi's group [16]. IRMOF-3 consists of Zn_4O clusters linked by 2-aminoterephthalic acid. Its crystalline structure is similar to the well known MOF-5 (or IRMOF-1); it consists of octahedral Zn_4O clusters linked by ditopic linear dicarboxylates [17] (Fig. 1a). However, all application work with this and similar MOF structures was either focused on gas adsorption [16], or on their use as intermediates for framework functionalization through the accessible non-coordinated amino groups [12,18]. Ingleson et al. [18] have demonstrated that the aromatic $-NH_2$ group interacts very easily with different solvents and its functionalization may trigger metal complex binding. Besides, the optimized geometry for IRMOF-3 shows that the benzene ring lies in-plane with the Zn_4O ring and this configuration is stabilized by an intramolecular hydrogen bond between the aromatic amino hydrogen atom and a carboxylate oxygen atom [19]. These findings suggest that IRMOF-3 and similar structures are interesting candidates for basic catalysis, since the reactivity of the amino group inside the MOF may be affected through these interactions.

In addition to IRMOF-3, other stable MOFs can be considered. Here we report the synthesis of a new structure based on MIL-53(Al) using 2-aminoterephthalic acid as linker. The MIL-53 series is built up from infinite chains of corner-sharing $MO_4(OH)_2$ ($M = Al^{3+}$ or Cr^{3+}) or $V^{4+}O_6$ octahedra interconnected by dicarboxylate groups resulting in a 3-D metal-organic framework containing 1-D diamond-shaped channels with pores of free diameter close to 7.5 Å (see Fig. 1b). The synthesis of a MOF with the MIL-53 structure and aminoterephthalic acid as linker has been very recently claimed by [20], named USO-1-Al. However, no proof (XRD, IR, elemental analysis) of the formation of such structure was provided so far.

The liquid-phase Knoevenagel condensation between a C=O functionality and an activated methylene group is an interesting classic route to C–C coupling for the preparation of important intermediates in the pharmaceutical industry and is often used as a test reaction for probing the activity of various solid base catalysts [21–26]. In fact, reacting benzaldehyde with compounds containing active methylene groups with different pK_a values, such as ethyl cyanoacetate ($pK_a \leqslant 9$) or ethyl acetoacetate ($pK_a \leqslant 10.7$) makes it possible to evaluate the basic strength of a catalyst.

The reaction may proceed according to two different mechanisms that depend essentially on the nature of the catalytic material used as solid base. For strong bases, direct deprotonation of the methylene group on the catalyst surface and reaction of the deprotonated intermediate with the slightly acidic benzaldehyde takes place, leading to the product.

When weaker bases, such as amino groups are involved in the catalytic process, formation of an imine intermediate occurs with the benzaldehyde (Schiff base, cycle 1 in Scheme 1). As consequence of the higher basicity of the formed benzaldimine compared to the free amine, the deprotonation of the methylene group takes places followed by reaction, regenerating the active site. The active methylene group can also react directly with the amino groups to form amides (Reaction 2 in Scheme 1), inhibiting then the interaction amine–benzaldehyde and causing the deactivation of the catalyst. Evidence for the formation of imine functionalities over modified silicas in the liquid phase using infrared spectroscopy have been recently reported [23].

In this paper, MOFs with basic groups similar to aniline ($pK_a = 4.6$) have been tested in the Knoevenagel condensation between benzaldehyde and ethyl cyanoacetate ($pK_a \leqslant 9$) and ethyl acetoacetate ($pK_a \leqslant 10.7$; Scheme 2), demonstrating an enhanced performance of the aromatic amine group, resulting in activities comparable to the best *state-of-the-art* solid bases, but without their deactivation due to leaching.

2. Experimental

2.1. General information

All chemicals were obtained from Sigma–Aldrich and were used without further purification. Inductively coupled plasma (ICP) emission spectrometry (Perkin–Elmer Optima 3000dv ICP-OES spectrometer) was used for the analysis of the bulk chemical composition of the synthesized MOFs. The crystalline materials were analyzed by X-ray diffraction (XRD) using a Bruker-AXS D5005 with Cu$K\alpha$ radiation. Scanning electron microscopy (SEM) on a Philips XL20 (15–30 kV) microscope was used to determine crystal morphology and size of the products. Thermogravimetric analysis of the MOFs was performed by means of a Mettler Toledo

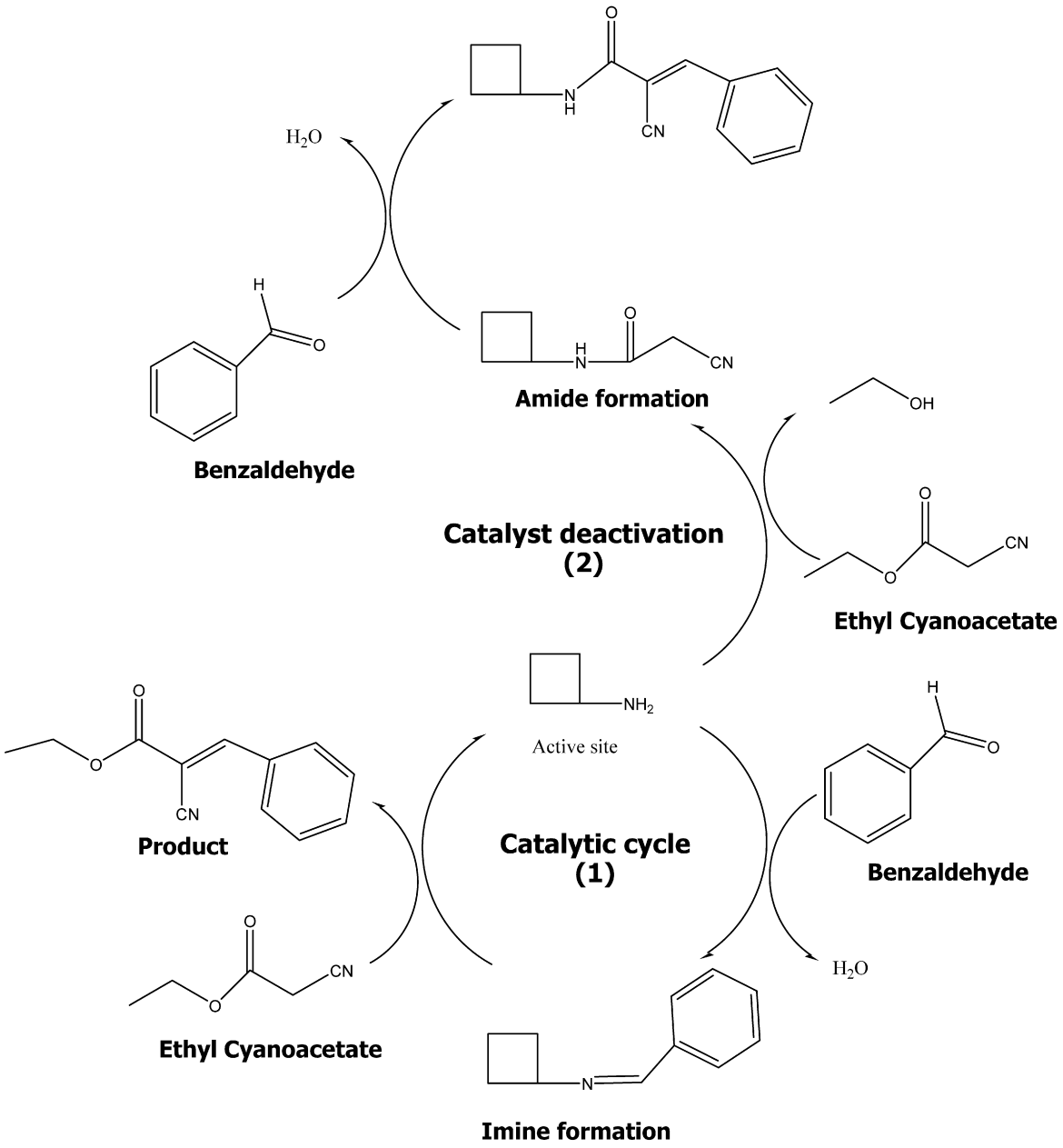

Scheme 1. Reaction mechanisms for the Knoevenagel condensation via imine intermediate (catalytic cycle 1) and catalyst deactivation via amide formation (pathway 2).

TGA/SDTA851e, under flowing N_2 at heating rates of 10 K/min. Nitrogen adsorption at 77 K in a Micromeritics ASAP 2010 gas adsorption analyzer was used to determine the textural properties of the MOFs. Elemental analyses of the solid samples were performed by Mikroanalytisches Labor Pascher (Remagen, Germany). DRIFT spectra were recorded in a Thermo Nicolet Nexus spectrometer, equipped with a liquid N_2-cooled MCT detector and a DRIFT high-temperature cell with CaF_2 windows. The spectra were registered after accumulation of 64 scans and a resolution of 4 cm^{-1}. A flow of helium at 30 mL min^{-1} was maintained during the measurements. Before collecting the spectra the different samples were pretreated under helium flow at 393 K for 1 h.

2.2. Catalyst synthesis

The synthesis of the IRMOF-3 catalysts was adapted from [27]. Dimethylformamide (DMF) and diethylformamide (DEF) were used as solvent. The resulting MOFs are referred to as IRMOF-3_{DMF} and IRMOF-3_{DEF}, respectively.

2.2.1. IRMOF-3_{DEF}

For the synthesis of IRMOF-3_{DEF}, zinc nitrate hexahydrate (61 mmol) and 2-aminoterephthalic acid (20 mmol) were dissolved in 500 mL of DEF in a 600 mL Erlenmeyer flask equipped with a pressure-releasing device. The reaction mixture was heated in a circulated air oven at 363 K for 24 h to yield large, cube-shaped crystals. The reaction vessel was then removed from the oven, allowed to cool to room temperature and transferred to a nitrogen-filled glove box. The solvent was decanted, and the remaining solid washed six times with 50 mL of anhydrous DMF, each time letting the solid soak in DMF for 8 h. Subsequently, the solid material was washed six times with 50 mL of anhydrous CH_2Cl_2, again each time soaking in CH_2Cl_2 for 8 h. After the final CH_2Cl_2 washing, the solvent was decanted and the sorbed CH_2Cl_2 was removed under reduced pressure for 12 h. The final product was a cube-shaped

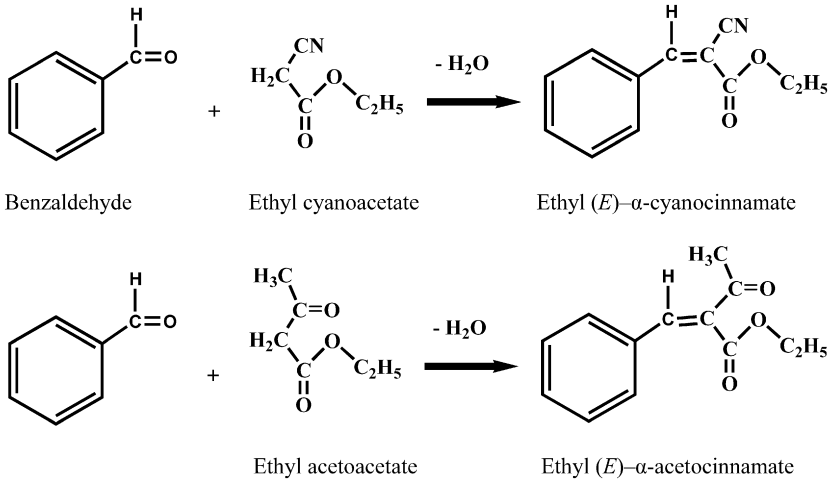

Scheme 2. Knoevenagel condensation of benzaldehyde with ethyl cyanoacetate and ethyl acetoacetate.

light-yellow material (yield ~70% based on 2-aminoterephthalic acid).

2.2.2. IRMOF-3_{DMF}

For the synthesis of IRMOF-3_{DMF}, two different synthesis scales were used: 100 and 500 ml, yielding IRMOF-$3_{DMF\,SB}$ and IRMOF-$3_{DMF\,LB}$ (Small and Large Batch).

For the synthesis of the IRMOF-$3_{DMF\,LB}$ zinc nitrate hexahydrate (15 mmol) and 2-aminoterephthalic acid (5 mmol) were dissolved in 490 mL of DMF and 10 mL H_2O in a 600 mL Erlenmeyer flask equipped with a pressure-releasing device. The reaction mixture was heated in an oven at 373 K for 24 h, yielding cube-shaped crystals. The product was processed and activated using the same procedure described above, yielding pale yellow cube-shaped crystals (yield ~90% based on 2-aminoterephthalic acid).

IRMOF-$3_{DMF\,SB}$ was synthesized using the same molar ratios as for IRMOF-$3_{DMF\,LB}$ but the syntheses were carried out in smaller (120 mL) Erlenmeyer flasks.

2.2.3. Amino-MIL-53(Al)

The synthesis of amino-MIL-53(Al) was adapted from [28]. 2.10 mmol aluminum nitrate nonahydrate dissolved in 15 mL DMF and 3.12 mmol 2-aminoterephthalic acid dissolved in 15 ml DMF were mixed in a Teflon insert and placed in an autoclave. The autoclave was heated in an oven at 403 K for 3 days. The yellow gel product was filtered off and washed with acetone. After removal of the acetone under reduced pressure, the product was washed overnight with methanol under reflux and dried at 110 °C under *in vacuo* for 8 h (yield ~40% yellow powder based on 2-aminoterephthalic acid).

2.3. General procedure for the Knoevenagel condensation reaction

In a typical batch experiment, an amount of the basic catalyst corresponding to 0.2 mmol of $-NH_2$ groups (based on the total amount of amino groups in the MOF) was added to a solution of 7 mmol ethyl cyanoacetate or ethyl acetoacetate in 5 mL of solvent in an Erlenmeyer flask, while being stirred under inert atmosphere (N_2) to avoid oxidation. After temperature adjustment, benzaldehyde (8 mmol) was added, keeping the reaction mixture under a static nitrogen atmosphere. The reaction mixture was periodically analyzed by gas chromatography using a Chrompack GC CP9001 equipped with an FID detector and a 60 m RTX®-1 (1% diphenyl-, 99% dimethylpolysiloxane) fused silica capillary column. The analysis was carried out directly after sampling to avoid any additional conversion in the reaction mixture.

Table 1
Unit cell formula, BET(N_2) area and micropore volume (calculated from *t*-plot) of the different MOFs.

	Unit cell formula	S_{BET} (m^2/g)	Micropore volume (cm^3/g)
IRMOF-3_{DEF}	$Zn_4(O)(CO_2–H_2NC_6H_3–CO_2)_3$	3683	1.74
IRMOF-$3_{DMF\,SB}$	$Zn_4(O)(CO_2–H_2NC_6H_3–CO_2)_3$	3130	1.16
IRMOF-$3_{DMF\,LB}$	$Zn_4(O)(CO_2–H_2NC_6H_3–CO_2)_3$	2440	1.02
Amino-MIL-53(Al)	$Al(OH)[O_2C–C_6H_3NH_2–CO_2]$	675	0.22

Reference experiments (blank runs) were performed for the different solvents (ethanol, DMSO, toluene, DMF, all HPLC grade) and temperatures (313, 333 and 353 K) studied. Experiments were performed by external agitation (shaking) instead of using internal stirring in order to avoid attrition of the particles and to facilitate the reuse of the different catalysts. After recovering the catalyst, it was washed overnight in DMF at 353 K, filtered and reused.

TOFs and number of turnovers based on the total number of amino groups present in each catalyst were calculated from the first reaction data points in the batch experiments (after reaction minutes).

3. Results

3.1. Characterization of the catalysts

Table 1 shows the BET specific surface areas and molecular cell formulas of the different MOFs, while Fig. 2 shows SEM micrographs and XRD analyses.

The specific surface area of the IRMOF-3_{DEF} is larger than both IRMOF-3_{DMF} samples, consistent with literature [27]. However, an influence of the synthesis scale was found for the IRMOF-3_{DMF} samples. For the smaller batch a larger specific surface area was obtained. This effect was not observed when using DEF as solvent. In general, the obtained specific surface areas exceed by far the best results reported in the literature for IRMOF-3 [29]. This can be attributed to the milder temperature conditions used in this work and with the improved workup procedure, adapted from a later publication of Yaghi's group [27].

For the amino-MIL structure, the BET specific surface area is also very similar to its terephthalic acid counterpart, known as MIL-53 [30] and smaller than the one reported for USO-1-Al. This is attributed to differences in the synthesis procedure, whereas Arstad et al. [20], using very similar synthesis conditions, claim the formation of a MIL-53 structure in 24 h, it took us 72 h to get such structure. It is well known that similar synthesis concentrations

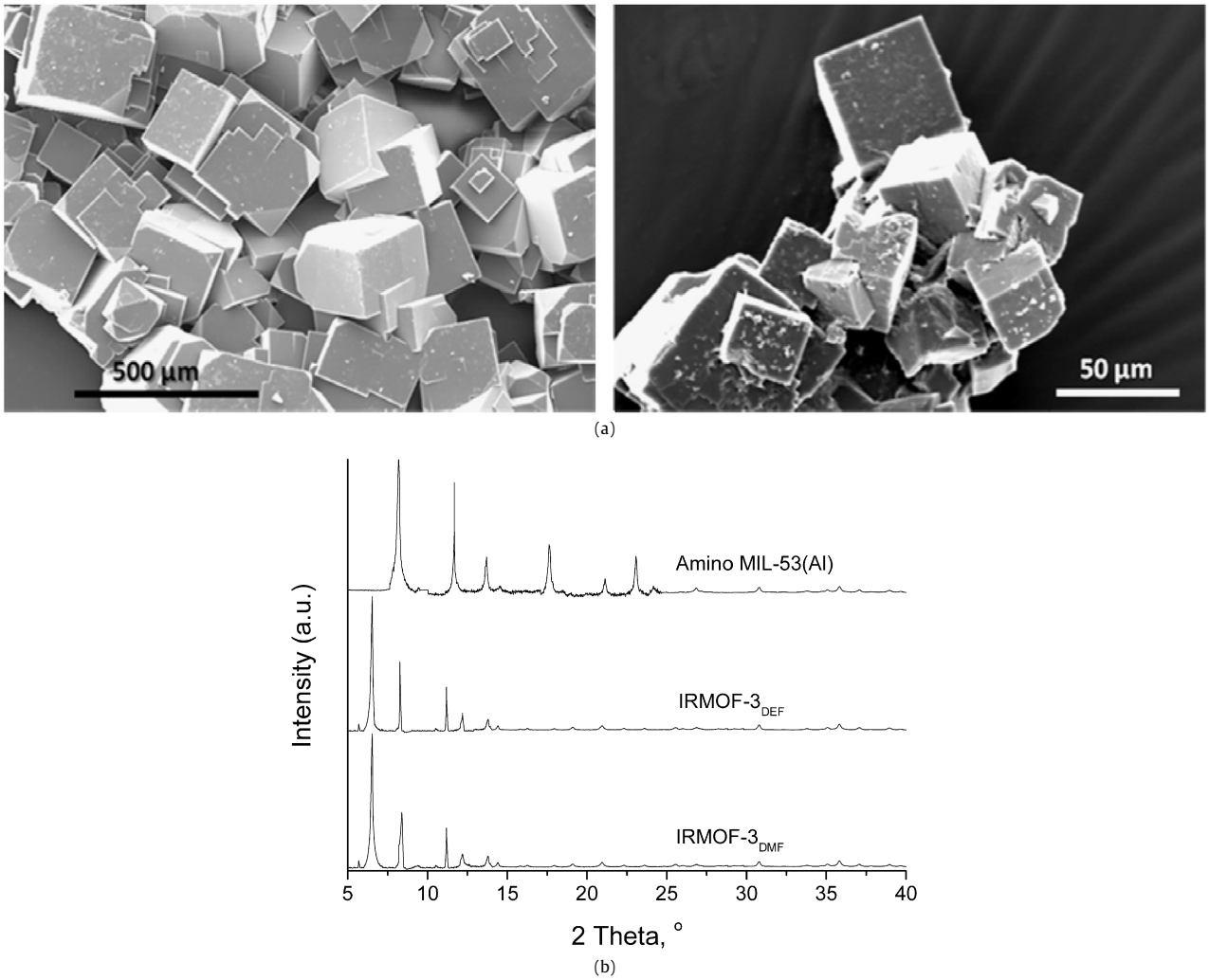

Fig. 2. (a) SEM micrographs of the IRMOF-3 samples: $IRMOF_{DEF}$ (left) and $IRMOF\text{-}3_{DMF\,LB}$ (right). (b) XRD patterns of the synthesized MOFs.

can yield to very different MIL structures, for instance MIL-101 and MIL-53 can be synthesized starting from the same synthesis mixture, at the same temperature, just by changing the synthesis time (24 h for MIL-101 and 72 h for MIL-53) [31]. In this sense, it has been very recently demonstrated that MIL-53 is the thermodynamically stable phase while MIL-101 is the kinetically favored phase [31]. Since no characterization data are given for the USO-1-Al MOF, it is hard to judge whether this structure and the here reported amino-MIL-53 are the same or not.

Cube shaped crystals are obtained for both IRMOF-3 samples, but much larger crystals are obtained when using DEF as solvent.

The XRD analyses shown in Fig. 2 show that there is hardly any difference between the IRMOF-3 samples and their patterns are very similar to those reported in the literature [12,18]. Peaks seem to be slightly better defined in the case of the sample synthesized in DEF. In the case of the amino-MIL-53, crystals suitable for single crystal X-ray crystal structure determination could not be obtained. However, the main reflections correspond well with those reported in the literature for Al(III) and Cr(III) MIL-53 [30,32]. To check whether or not the structure of the firstly reported amino-MIL-53(Al) corresponded with the expected one, elemental analysis was performed on the sample. The found composition (wt%) for the dried material was: C: 48.6, H: 3.5, O: 33.9, N: 4.5, Al: 8.25. The obtained N/Al ratio in the MOF (0.54) fits well the expected one (0.52).

Further characterization of the synthesized MOFs was performed by means of IR spectroscopy. Fig. 3 shows the DRIFT spectra corresponding to the $IRMOF\text{-}3_{DMF\,SB}$ and the amino-MIL-53(Al). In both cases, bands at 3370 and 3490 cm^{-1} correspond with the symmetric and asymmetric stretching of primary amines, which demonstrates that the amino groups are free for interaction in both structures. For the amino-MIL-53, the hydroxyl groups of the trans corner sharing octahedra $AlO_4(OH)_2$ chains give rise to a $\nu_{(OH)}$ band at 3700 cm^{-1} with a shoulder near 3660 cm^{-1}, similarly as reported for MIL-53(Cr) [33], but shifted 50 cm^{-1} to lower wavenumbers. This fact would indicate OH groups with a stronger basicity in the amino-MIL-53(Al).

Surface basicity was studied by FTIR after adsorption of CO_2. CO_2 adsorption followed by DRIFTS is a powerful technique for characterization of basic solids [34], especially when other techniques like CO_2 TPD [2] or using Hammet indicators [35] cannot be applied either because of limited thermal stability or because the pores of the material are too small to allow interaction with bulky molecules. CO_2, an electron acceptor, is expected to act as a Lewis acid. Its adsorption on the different MOF samples was studied by means of DRIFTS in order to check whether or not the synthesized MOFs possess basic sites available for interaction. Results after subtracting the MOF background are presented in Fig. 4.

In the case of the IRMOF-3, in the ν_2 range (CO_2 bending mode), two bands at 669 (with a shoulder at 667 corresponding to the gaseous phase CO_2) and 653 cm^{-1} are observed. The pres-

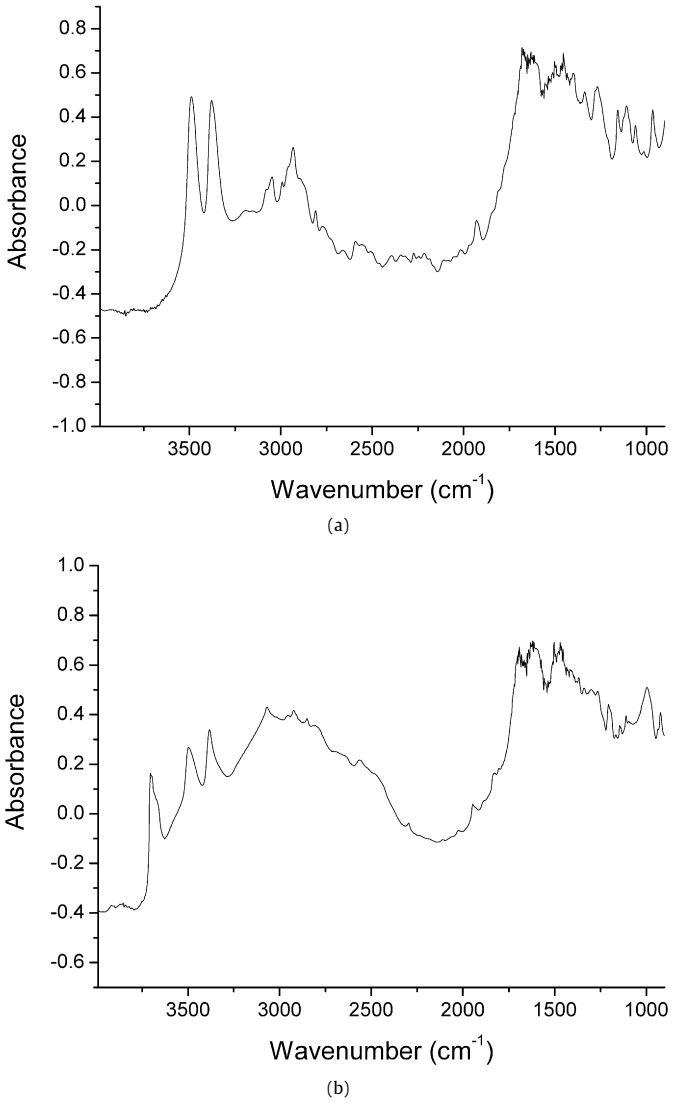

Fig. 3. DRIFTs spectra of IRMOF-3 (a) and amino-MIL-53(Al) (b).

ence of a double band for the ν_2 stretching mode of CO_2, indicates a lowering of the symmetry upon adsorption, and was firstly reported in a MOF (MIL-53) by [33]. Although this could be due to some confinement effect inside the micropores of the material, no ν_2 splitting has been observed in other micro- and mesoporous materials such as ZSM-5 zeolites or MCM-41 [36]. In general, this kind of splitting is common in the case of electron donor–acceptor (EDA) complexes of CO_2 with molecules such as pyridine, alcohols or functional groups of polymers and is due to the interaction of CO_2 via the carbon atom as an electron acceptor [33]. The high and low ν_2 frequency bands are assigned to the out-of plane and in-plane bending modes, respectively [37]. In the case of IRMOF-3, the intensity of both bands is very similar, suggesting that there is only one type of adsorbed species.

In the case of the amino-MIL-53(Al), the interaction of CO_2 with the framework seems to be more complex. Four bands at 669, 661, 655 and 649 cm^{-1} are observed. Two bands (655 and 669 cm^{-1}) correspond with the observed CO_2 adsorption in IRMOF-3 and the other two bands (661 and 649 cm^{-1}) correspond with previous observations for MIL-53 [33], without amino groups. This strongly suggests the adsorption of CO_2 in two different ways, forming EDA complexes with both $-NH_2$ and –OH groups of the structure.

The high and low ν_2 frequency bands, assigned to the out-of plane and in-plane bending modes, respectively, should lead to a ν_3 frequency lower than that observed in the gas phase (2349 cm^{-1}), which is also expected in the case of EDA complexes involving CO_2 as an electron acceptor [37]. Due to the relatively low CO_2 partial pressure used during the experiments (compared to the literature), this band is only slightly visible for the amino-MIL-53(Al) sample (2334 cm^{-1}).

In addition, several new peaks can be observed in the range 1000–1700 cm^{-1}. Amines may react with CO_2 to form carbamate species [34]. The latter are in equilibrium with the carbamic acid species (DRIFT peaks around 1450 cm^{-1}). Carbamate species can react with adsorbed water or surface hydroxyl groups forming carbonates, bicarbonates or formates. In fact, the broad band appearing at 1029 cm^{-1} in the amino-MIL-53(Al) may be related to the formation of hydrogen carbonates (ν_{CO_3} vibration) [38] due to the interaction of CO_2 with the hydroxyl groups of the MOF.

3.2. Catalytic testing

3.2.1. Performance in DMF

The performance of the different MOFs as basic catalysts was tested with the Knoevenagel condensation reaction of benzaldehyde and ethyl cyanoacetate in the presence of different solvents at 313 and 333 K, using a 2/100 molar ratio of amino groups in the MOF to the amount of ethyl cyanoacetate reactant. Experiments performed at room temperature showed high conversions, but due to a strong adsorption of the product (ethyl (*E*)-α-cyanocinnamate) in the MOF, product yields could not be accurately calculated. Experiments without solvent were also performed, but the high reaction rate led to precipitation of the product within the framework, and following the progress of conversion with time was not possible. The graphs presented in Figs. 5, 6 and 8 to 10 show the yields of ethyl (*E*)-α-cyanocinnamate based on the ethyl cyanoacetate conversion (100% selectivity was achieved in every case) as a function of time.

Fig. 5 shows the performance of IRMOF-$3_{DMF\,LB}$ when the reaction is performed in presence of DMF as solvent at 333 K together with the results obtained for the blank run. Results obtained using aniline as homogeneous basic catalyst are included for comparison, resembling most the aromatic amino functionality in the MOFs based on 2-aminoterephthalic acid. IRMOF-$3_{DMF\,LB}$ exhibits a higher activity than aniline. Taking into account that the total amount of amino groups was equal in both cases, it seems that the reactivity of the amino groups is enhanced after incorporation in the MOF structure.

Fig. 6 shows the performance comparison in DMF as solvent of the two different IRMOF-3_{DMF} and the IRMOF-3_{DEF} samples at 313 K. The higher activity of the IRMOF-3_{DEF} and IRMOF-$3_{DMF\,SB}$ correlate with their larger specific surface area, indicative of a better accessibility of the amino groups inside the structure. Since IRMOF-3_{DEF} crystals are much bigger than the IRMOF-3_{DMF} samples, experiments with crushed IRMOF-3_{DEF} were also performed, obtaining the same results as with the uncrushed crystals (not shown). These results point out that diffusion limitation are absent in spite of the huge crystal size of this most active sample.

The evolution in the concentration of the reactants with time for the experiment with the amino-MIL-53 sample at 313 K is shown in Fig. 7. Although adsorption of reactants can be noticed, no product formation could initially be detected. The concentration of the product in the liquid phase is even smaller than in the blank experiments, which would suggest a strong adsorption of the product inside the MOF pores. In order to check whether the sample was active or not, after 150 min, the temperature was increased to 353 K in order to stimulate desorption of components from the

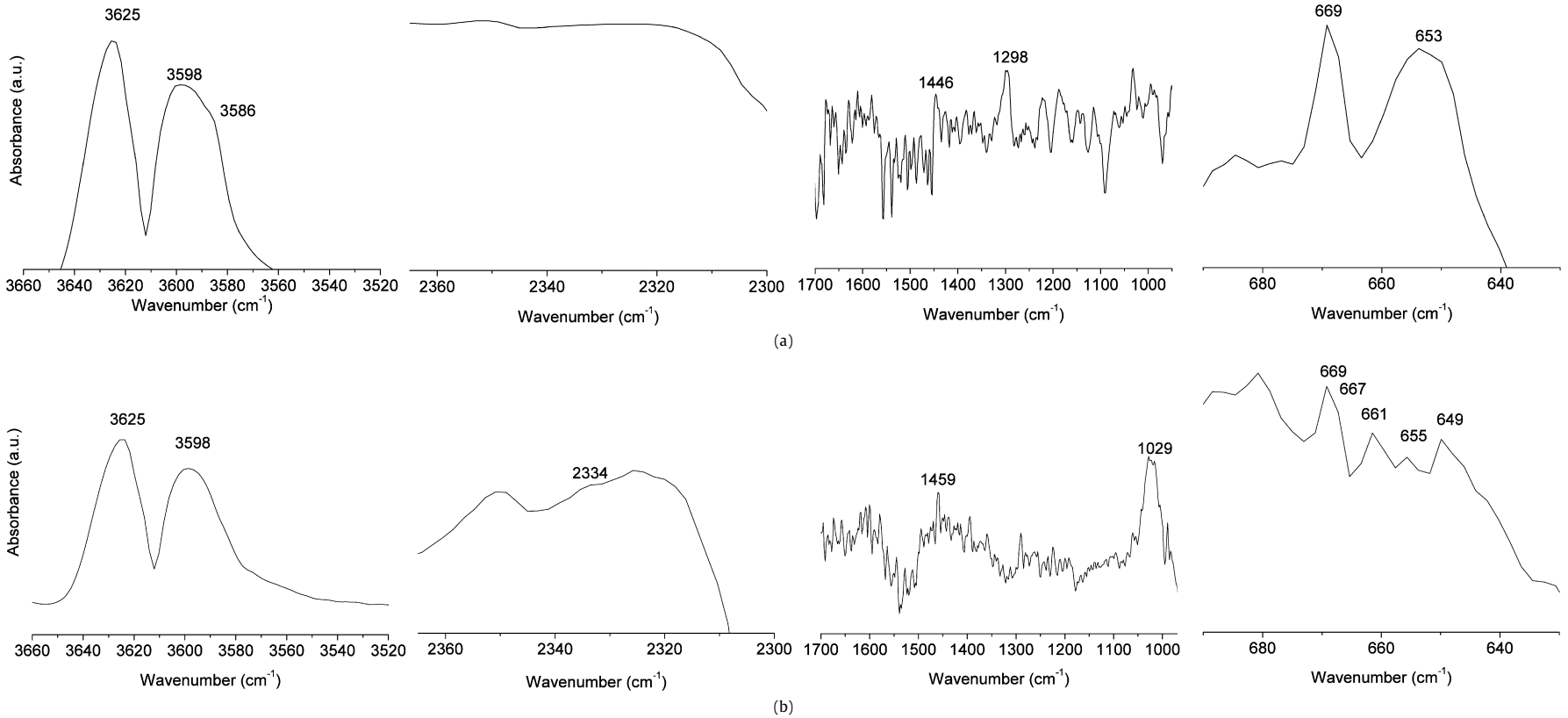

Fig. 4. DRIFTs spectra of activated IRMOF-3 (a) and amino-MIL-53(Al) (b) after introduction of CO_2 into the cell.

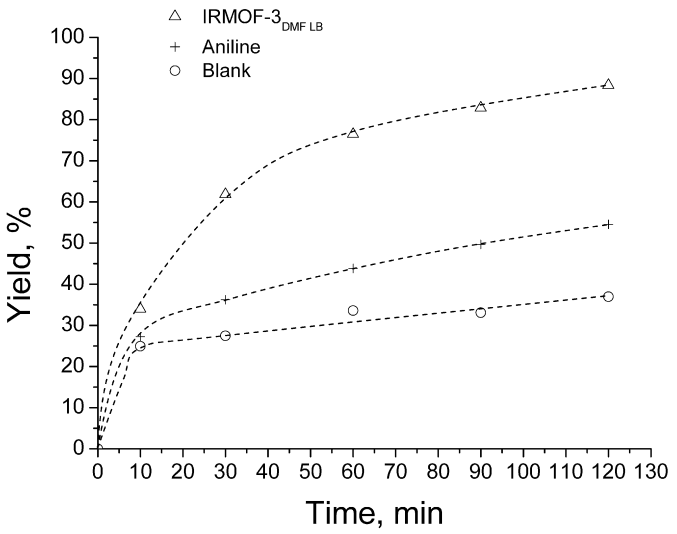

Fig. 5. Knoevenagel condensation of benzaldehyde (8 mmol) and ethyl cyanoacetate (7 mmol) in DMF (5 ml) at 333 K: comparison between the performance of IRMOF-$3_{DMF\,LB}$ (0.06 mmol: corresponds to 0.18 mmol of $-NH_2$ groups) and aniline (0.2 mmol).

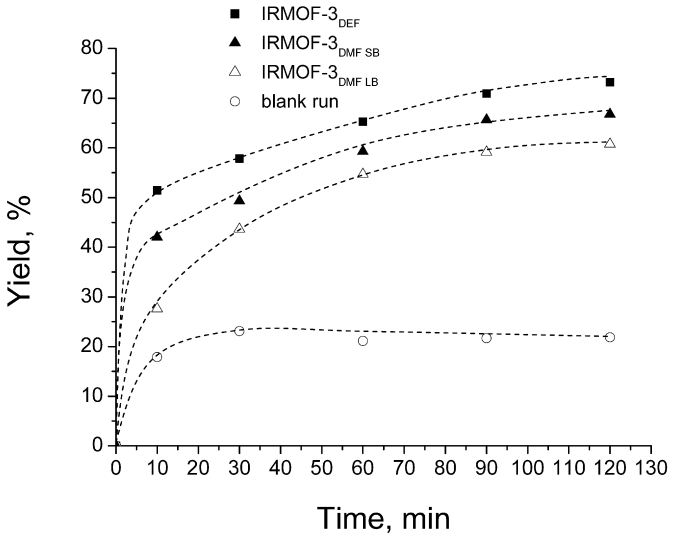

Fig. 6. Knoevenagel condensation of benzaldehyde (8 mmol) and ethyl cyanoacetate (7 mmol) in DMF (5 ml) at 313 K: comparison between the performance of IRMOF-$3_{DMF\,LB}$ (0.06 mmol: corresponds to 0.18 mmol of $-NH_2$ groups) and IRMOF-3_{DEF} (0.06 mmol: corresponds to 0.18 mmol of $-NH_2$ groups).

MOF structure. After this increase in temperature, the appearance of the product in the liquid phase can be observed.

To determine if leaching and/or permanent deactivation of the catalyst occur, the IRMOF-3 catalyst samples were reused several times. The reactions were carried out in DMF at 313 K using the same molar ratios. When the reaction was completed after 2 h, the solid was filtered off, washed with DMF overnight at 353 K, thoroughly washed with CH_2Cl_2 and reused in a second and third run. A minor decrease in activity was observed after the first run (Fig. 8). No further activity loss was observed when considering the small amount of catalyst lost during the recycling process. In addition, the reproducibility of the experiments can be judged by comparing runs 1 and 1' in Fig. 8b. To determine whether or not leaching of active sites takes place the same reaction was performed during 30 min, at this point the catalyst was removed by hot filtration and the evolution of products formation was followed maintaining the same reaction conditions. Results for IRMOF-$3_{DMF\text{-}LB}$ are shown in Fig. 8c. No further reaction takes

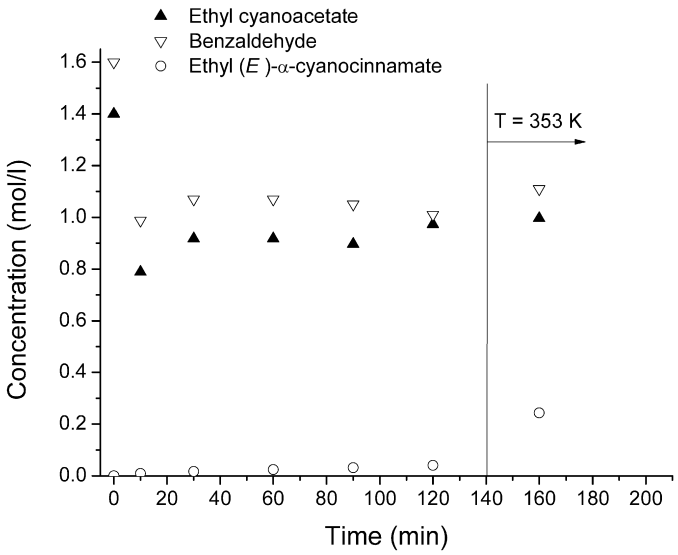

Fig. 7. Knoevenagel condensation of benzaldehyde (8 mmol) and ethyl cyanoacetate (7 mmol) in DMF (5 ml) at 313 K catalyzed by the amino-MIL-53 (0.2 mmol): evolution of reactants and product concentration in the liquid phase.

place after removing the catalyst from solution, demonstrating the absence of active sites leaching.

3.2.2. Solvent dependence

In case of homogeneous basic catalysts, the character of the solvent used may have a strong effect on the reaction rate due to several reasons:

- Polarity: usually, the higher the polarity the faster the reaction rate [4,25]. This behavior is attributed to the influence of the solvent on the transition state and to a change in the capacity of the catalyst for proton transfer: when polar reagents are involved, the transition-state complex is better solvated by polar solvents and the partition of the reactants at the solid–liquid interface is higher, decreasing the activation free enthalpy and enhancing the reaction rate.
- Amphiprotic properties, some protic solvents such as ethanol may also enhance the activation of the slightly acid benzaldehyde, yielding a higher catalytic activity.

The influence of the solvent on the reaction rate for the MOF catalyzed reaction between benzaldehyde and ethyl cyanoacetate was investigated for solvents with different dielectric constants (ε) and amphiprotic properties: DMSO ($\varepsilon = 48.9$), DMF ($\varepsilon = 36.7$), EtOH ($\varepsilon = 24.3$), cyclohexane ($\varepsilon = 18.5$) and toluene ($\varepsilon = 2.4$). The dielectric constant can be considered as a measure of polarity. Results for IRMOF-$3_{DMF\,LB}$ are shown in Fig. 9. DMSO proved to be the most active solvent for the reaction, while experiments in toluene revealed hardly any activity of the MOFs. In spite of its lower dielectric constant, the catalytic performance in ethanol was better than in DMF.

3.2.3. Effect of the reactant addition order: Catalyst deactivation?

As mentioned in the introduction, it has been proposed that the order of addition of the reactants may play a role during the Knoevenagel condensation: ethyl cyanoacetate may react with some of the amino groups of the catalyst to form amides, inhibiting then the interaction amine–benzaldehyde and causing deactivation of the catalyst [23].

To check if this applies to the studied catalysts, the order of reactants addition was changed during the Knoevenagel condensation on the IRMOF-$3_{DMF\,SB}$. If the proposed mechanism is

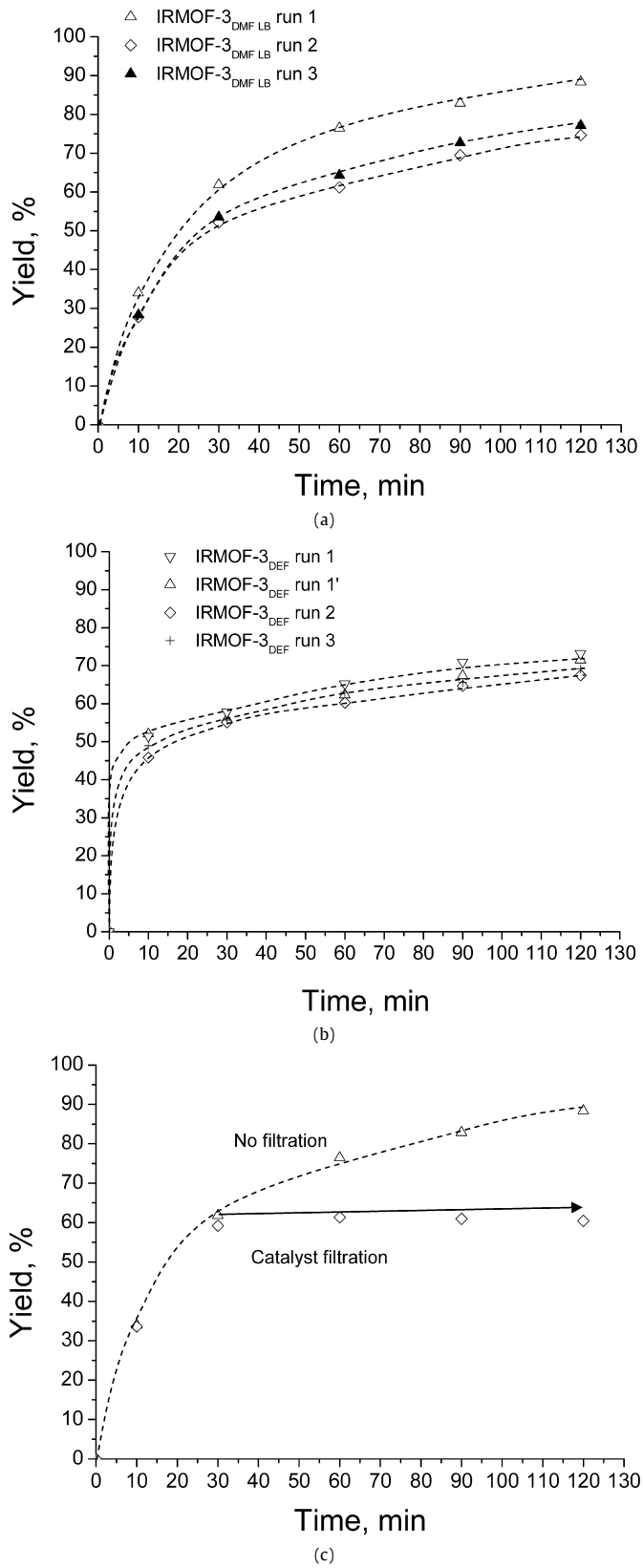

Fig. 8. Knoevenagel condensation of benzaldehyde (8 mmol) and ethyl cyanoacetate (7 mmol) in DMF (5 ml) for repeated runs with the same catalyst sample: (a) at 333 K catalyzed by IRMOF-$3_{DMF\,LB}$ (0.06 mmol: corresponds to 0.18 mmol of $-NH_2$ groups). (b) at 313 K catalyzed by IRMOF-3_{DEF} (0.06 mmol: corresponds to 0.18 mmol of $-NH_2$ groups) for several reaction cycles. (c) the same reaction as in (a) was performed during 30 min, at this point the catalyst was removed by hot filtration and the evolution of products formation was followed maintaining the same reaction conditions.

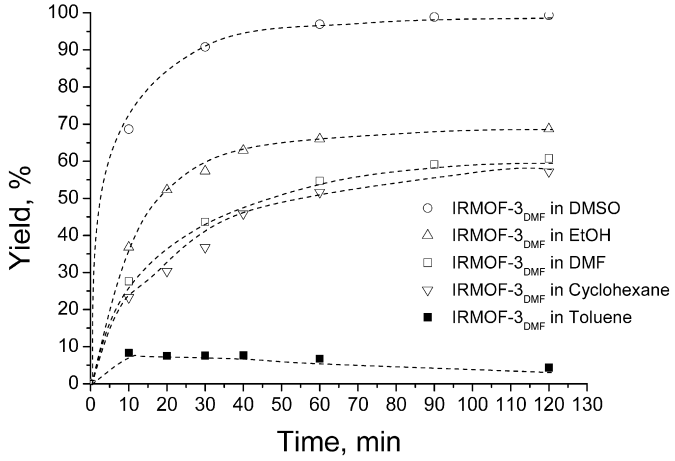

Fig. 9. Knoevenagel condensation of benzaldehyde (8 mmol) and ethyl cyanoacetate (7 mmol) in different solvents (5 ml) at 313 K catalyzed by IRMOF-$3_{DMF\,LB}$ (0.06 mmol: corresponds to 0.18 mmol of $-NH_2$ groups).

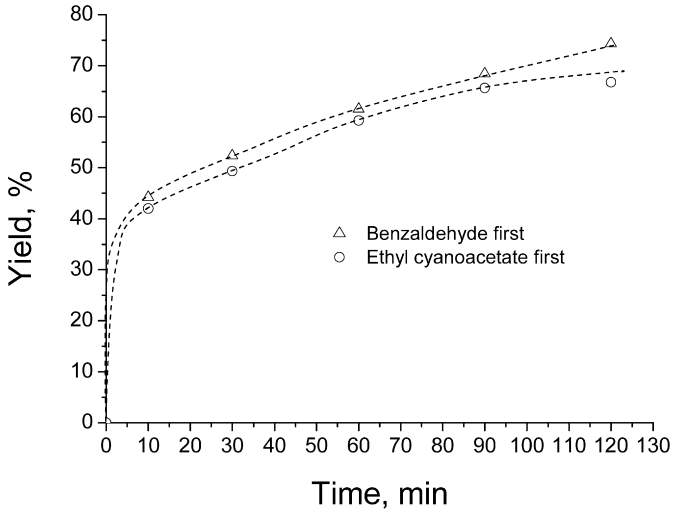

Fig. 10. Knoevenagel condensation of benzaldehyde (8 mmol) and ethyl cyanoacetate (7 mmol) in DMF (5 ml) at 333 K catalyzed by IRMOF-$3_{DMF\,SB}$ (0.06 mmol: corresponds to 0.18 mmol of $-NH_2$ groups) changing the order of reactants addition.

applicable in this case, a higher conversion would be expected when adding first benzaldehyde, since an inhibiting effect of ethyl cyanoacetate would be suppressed. Fig. 10 shows the results for the two addition orders. Although during the first reaction hour hardly any difference can be observed, it seems that reaction keeps running slightly faster after 120 min when benzaldehyde is added first. This can indeed be due to some inhibiting effect of the active methylene group. Although it has been shown that the formation of the benzaldimine intermediate is faster than the rate of formation of the amide via ethyl cyanoacetate [23], the slow formation of such amide might slowly block the active sites.

DRIFT spectra were collected at different times during the adsorption of solutions of ethyl cyanoacetate or benzaldehyde in DMSO using similar concentrations as during the reaction experiments at room temperature. Fig. 11a presents the spectrum collected after 60 min of contact between IRMOF-3_{DEF} with a solution of ethyl cyanoacetate in DMSO. Besides the characteristic signals of dissolved ethyl cyanoacetate in DMSO at 1749 and 1308 cm^{-1}, no new bands evolve in the 1200–1800 cm^{-1} range, where amide vibrations should be present, as observed for amino-modified silica [23]. So no clear evidence of a significant amide

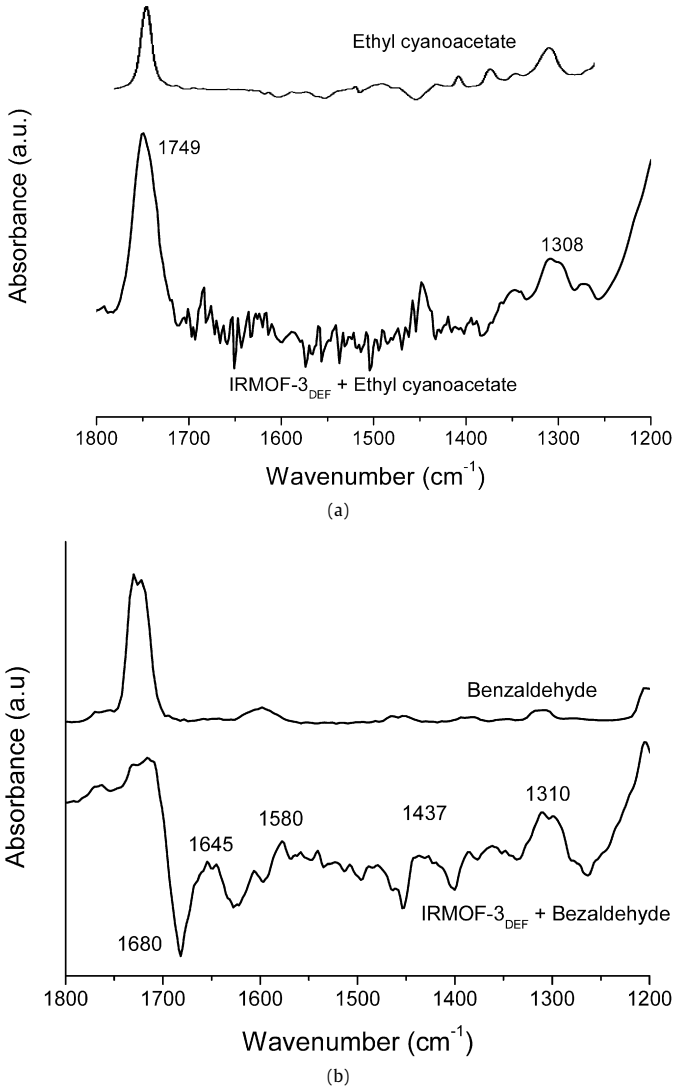

Fig. 11. DRIFTs spectra of activated IRMOF-3 after 60 min of contacting a solution of ethyl cyanoacetate (a) or benzaldehyde (b) in DMSO (1.4 mol/l) at room temperature.

formation, which may account for site blocking (Scheme 1), could be extracted from this experiment. Fig. 11b shows the spectrum of the IRMOF-3_{DEF} catalyst after contact with a solution of benzaldehyde (BA) for about 60 min. A strong absorption is observed at 1645 cm^{-1} which is accompanied by absorptions at 1580 and 1440 and 1310 cm^{-1} and by a negative feature centered at about 1680 cm^{-1}. The difference between this spectrum and that of benzaldehyde in solution is obvious. Reaction between benzaldehyde and the surface amino groups occurs, with the most prominent band at 1645 cm^{-1} being the (C=N) mode of the surface benzaldimine group (Scheme 1), which also shows vibrational modes associated with the phenyl ring (1580 and 1440 cm^{-1}).

3.2.4. Knoevenagel condensation of benzaldehyde and ethyl acetoacetate

To estimate the capacity of the IRMOFs to activate methylene groups with $pK_\alpha > 9$, the Knoevenagel condensation was performed of benzaldehyde with ethyl acetoacetate, a more demanding compound containing a methylenic group with a higher basic strength ($pK_\alpha = 10.7$). Fig. 12 shows the yield of the condensation product (ethyl (*E*)-α-acetocinnamate) vs. time when using IRMOF-$3_{DMF\,LB}$ as catalyst in DMSO at 313 and 353 K. As expected, the

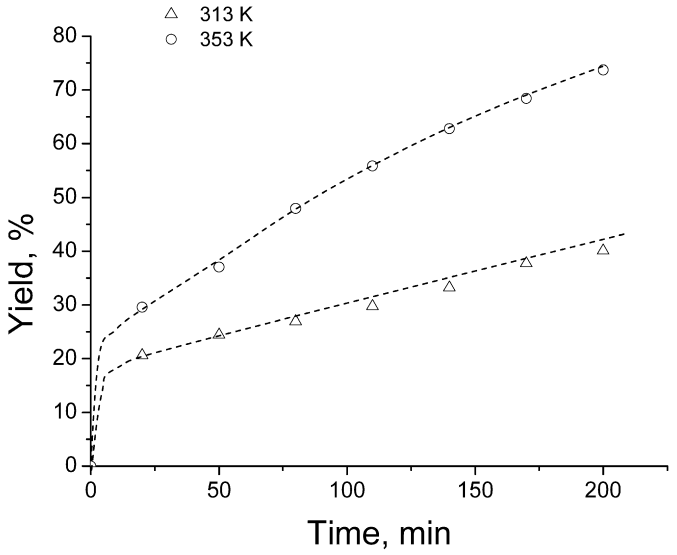

Fig. 12. Knoevenagel condensation of benzaldehyde (8 mmol) and ethyl acetoacetate (8 mmol) in DMSO (5 ml) at 313 K and 353 K catalyzed by IRMOF-$3_{DMF\,LB}$ (0.12 mmol: corresponds to 0.36 mmol of $-NH_2$ groups).

reaction rate is lower than in the case of ethyl cyanoacetate, but the levels of conversion are higher than those reported for other basic catalysts under similar conditions [26].

4. Discussion

The targeted amino containing MOFs have been synthesized successfully. Their composition is confirmed by elemental analysis, their structure by XRD (Fig. 2) and their amine functionality proven by IR spectroscopy (Fig. 3). The differences in the textural parameters for the IRMOF-3 (Table 1) are attributed to the synthesis method. The use of DMF as solvent in the synthesis increases the possibility of chain intergrowth or catenation [39], resulting in an interpenetrating network. The most immediate consequence of interpenetration is a reduction of the available space inside the framework, reducing the specific surface area and pore volume. Moreover, the accessibility of the active sites in the catalysts is reduced (vide infra).

Following the adsorption of an electron acceptor molecule like CO_2 on the studied metal-organic frameworks by IR spectroscopy demonstrates that both structures possess Lewis basic properties. In the case of the IRMOF-3 samples, only amine groups are acting as electron donors, while for the amino-MIL-53 (Al), also the hydroxyl groups of the trans corner sharing octahedra $AlO_4(OH)_2$ can act as basic center (Fig. 4).

From the reaction experiments, we conclude that MOFs based on 2-aminoterephthalic acid are highly active and stable basic catalysts for the Knoevenagel condensation. Compared to aniline, which, in principle, should yield a similar behavior under the same conditions, the incorporation of an aromatic amino in the open IRMOF-3 framework increases the activity of the amino group significantly over the whole reaction period. After 2 h of reaction at the same temperature, the conversion for the IRMOF-$3_{DMF\,LB}$ is almost double than that of aniline (Fig. 5). Furthermore, IRMOF-3_{DEF} has a higher productivity than IRMOF-$3_{DMF\,LB}$, in spite of its ~5 times larger particle size (Fig. 6).

The catalytic activity correlates with the specific surface area of the samples, and is attributed to the different accessibility of the active sites in the catalysts, mentioned above. Diffusion limitations in the experiments with the most active IRMOF-3_{DEF} catalyst are absent, as the results with crushed catalyst demonstrate.

Table 2
Selected studies on Knoevenagel condensation of benzaldehyde (B) and ethyl cyanoacetate (EC) or ethyl acetoacetate (EA) over solid catalysts.

Reference	Yield (%) after 2 h[a]	Temperature (K)	Solvent	Catalyst used	Initial TOF (min^{-1})[b]
This work	99 (EC) 58 (EA)	313 (EC) 353 (EA)	DMSO	IRMOF-3_{DEF}	2.9 (EC) 0.33 (EA)
[15]	80 (EC)	353	Cyclohexane	Ethyldiamine grafted MIL-101	0.37
[26]	~72 (EC) ~18 (EA)	298 (EC) 353 (EA)	DMSO	1,8-Bis(dimethylamino)-naphthalene (DMAN)	1.57 (EC) 0.06 (EA)
[4]	~80 (EC)	313 (EC)	Ethanol	DMAN supported on MCM-41	3
[44]	~70 (EC) ~38 (EA)	363 (EC) 393 (EA)	–	Amino-grafted Cs-exchanged NaX zeolite	–
[42]	41 (EC) (after 1 h)	298	Ethanol	Amine-modified pore-expanded MCM-41	2.6
[45]	50 (EC)	298	Toluene	Modified Mg-Al hydrotalcite	–
[22]	21 (EC)	413	–	Zn exchanged Hβ zeolite	–
[46]	52 (EC)	323	Toluene	Aluminophosphate oxynitrides	0.67
[47]	~85 (EC) (after 3 h)	373	–	Zeolite Y containing methylammonium cations	0.3
[11]	7 (EC)	298	Benzene	3-D porous coordination polymer	–

[a] Yield towards ethyl-α-cyanocinnamate (for EC) or ethyl-α-acetocinnamate (for EA) unless stated otherwise.
[b] TOF calculated after 10 reaction min (when available data).

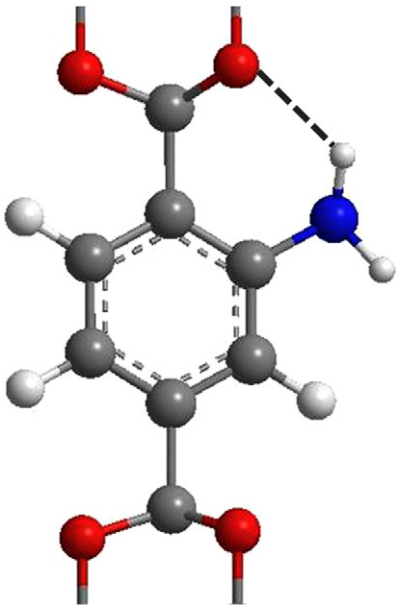

Fig. 13. Intramolecular hydrogen bond formed inside IRMOF-3 in its minimum energy configuration [19]. (Oxygen atoms in red, carbon atoms in gray, nitrogen atoms in blue and hydrogen atoms in white. For interpretation of the references to color in this figure legend, the reader is referred to the web version of this article.)

Table 2 shows a comparison of our results with different published studies on Knoevenagel condensations, demonstrating that the performance of IRMOF-3 is among the best state-of-the-art catalysts. The Turn-Over-Frequencies (TOFs) given are based on the initial data points (after 10 reaction min), assuming that all amino groups are active centers.

It has recently been proposed that in its optimized geometry, the benzene rings in IRMOF-3 lie in-plane with the zinc-oxocarboxylate rings and are stabilized by an intramolecular hydrogen bond between amino and a carboxylate oxygen [19] (Fig. 13). The formation of intraframework hydrogen bonding with an electron donating oxygen from the carboxylic group may increase the basic strength of the MOFs, favoring the formation of the benzyldimide intermediate by steric effects. Basicity enhancement effects have been reported for polyamines; the effect of molecular strain in the molecule on the Brønsted basicity of amines has been investigated for a long time. It appears that all strain effects on monoamines are base weakening, while in polyamines strain energy can be utilized to increase base strength [40]. For instance, aromatic diamines with neighboring nitrogen atoms at short distances, named 'proton sponges', show a well-defined and strong basicity [41]. Indeed, the IRMOF-3_{DEF} in our study shows a similar activity as the most active solid basic catalysts, like the 'proton sponges' immobilized on different inorganic carriers [4], pore expanded MCM-41 [42] or aminopropyl modified silica [23]. IRMOF-3 shows a much higher activity and a better stability than amino grafted MOFs [15], and exceeds by far the performance of other solids such as ion exchanged zeolites [22]. IRMOF-3 catalysts are able to catalyze reactions involving active methylene compounds with $pK_\alpha > 10$, which demonstrates the huge increase in basicity of the amino groups when incorporated inside the MOF structure. We attribute this high activity of the IRMOF-3 to the intramolecular hydrogen bond interaction between amino and an electron donating carboxylate oxygen [19] (Fig. 9), enhancing the basicity of the $-NH_2$ group. If aniline is used as catalyst, this kind of interaction is absent, and even if a higher concentration of amino groups is used in the reaction medium than with the IRMOF-3 catalyst, the yield of the product does not exceed much that of the blank runs without any amino groups present.

It must be noted that the initial conversion in blank runs was appreciable (see Figs. 3 and 4), an observation that has not often been reported in the literature [4,22,25,26,42]. Nevertheless, the activity of IRMOF-3 is considerably higher, and the yield develops to much higher levels, whereas that for the blank runs levels off rapidly.

When comparing the performance between the IRMOF-3 and amino-MIL samples, it is concluded that adsorption and diffusion phenomena play a key role in the poor performance of the amino-MIL sample. The 1-D pore structure (in contrast to the 3-D pore structure of IRMOF-3), together with the smaller pore diameter (7.3 vs 15 Å), results in single file diffusion phenomena, slowing down tremendously the transport in and out of the structure. The main region of activity will then be located at the pore mouth of the particles, similarly as for a 1-D pore structure in an acid zeolite like mordenite. The smaller pore size will also increase the Van der Waals interaction with the molecules resulting in a stronger adsorption of the product, as is observed. These properties make the amino-MIL-53 MOF not a suitable candidate for this reaction in terms of productivity, but its activity for this base catalyzed reaction is still demonstrated. In spite of all that, its use at higher temperatures or with smaller molecules, where diffusion limitations and strong adsorption should dominate less, or even its use in gas phase base catalyzed reactions might be considered.

Experimental evidences for the occurrence of the proposed reaction mechanism (Scheme 1) have been given. Formation of intermediate benzaldimine species is clearly observed. Moreover, although the order of reactants addition had a minor effect on the conversion, no proofs of amide formation via ethyl cyanoacetate could be collected when following the adsorption of this reactant by DRIFTs.

The polar solvent DMSO with the largest dielectric constant is the most effective for the formation of the product (Fig. 7), sim-

ilar as observations in the homogeneous phase [25,26]. This is attributed to the hydrogen bond acceptor power of DMSO, stabilizing the protonated form of the amino group, increasing the rate of proton transfer [4] and promoting in this way in the formation of the benzaldimine intermediate species. The faster reaction in EtOH than in DMF differs, however, from the trend in solvent polarity. This suggests that besides the increased rate of proton transfer, the different solvation power and consequently in the partition of the reactants at the solid–liquid interface plays a role [23]. The amphiprotic properties of ethanol may induce the electrophilic polarization of the carbonyl group of benzaldehyde (due to its moderated acid character) and enhance the reaction rate [26]. A nearly apolar solvent like toluene seems to affect negatively the catalytic performance of the MOFs, in clear contrast with results reported for other solid supported basic catalysts [4]. In the latter case the hydrophilic character of the support determines the performance of supported homogeneous catalysts [3,4]; the higher the hydrophobicity of the porous material, the less the effect of the solvent and the faster the diffusion of the products. Since IRMOF-3 is a hydrophilic solid (Zn atoms are not fully coordinated), it is not surprising that the polarity of the solvent has a large impact on the performance of the catalyst. Indeed, the results suggest that the affinities of benzaldehyde and ethyl cyanoacetate for toluene are higher than for other solvents and that this distribution between the solvent and the solid makes the reaction slower.

The IRMOF-3 samples are stable under the studied reaction conditions and their reuse is possible. This is not quite in line with the inherent moisture sensitivity reported for Zn_4O based metal-organic frameworks [27]. However, this moisture sensitivity has been reported without solvents being present inside the pores of the material. When high boiling point solvents are present, Zn_4O cluster solvation occurs [18,43], resulting in a hydrophobic barrier that protects the clusters from decomplexation by water, as might be the case in the present study.

The presented results demonstrate that by incorporating amino groups in a MOF-structure, highly active solid basic catalysts are obtained. Since the amino group is an intrinsic part of the organic linker in the MOF, and not grafted to the inorganic part, leaching [15] does not occur and a stable system results. This work may form the basis for further development of MOFs as heterogeneous catalysts, especially as solid basic catalysts, a field which is relatively underdeveloped compared to acid catalysis.

5. Conclusions

In this work, metal-organic frameworks with non-coordinated amino groups are shown to be active solid basic catalysts in the Knoevenagel condensation of benzaldehyde with two methylene active compounds of different pK_a, viz. ethyl cyanoacetate ($pK_a \leqslant 9$) and ethyl acetoacetate ($pK_a \leqslant 10.7$).

The activity of the IRMOF-3 depends on the specific surface area of the sample, determined by its preparation procedure. IRMOF-3_{DEF} shows an activity at least as high as the most active solid basic catalysts, with 100% selectivity to the condensation product. Diffusion limitations were absent for this catalyst.

The reaction has been shown to proceed through the formation of benzaldimine intermediates. The effect of the solvent on the reaction rate could be explained by both affinity and deprotonation capacity.

The performance of the amino-IRMOF in different solvents resembles more homogeneous catalysts' behavior rather than that of other solid basic catalysts.

One new MOF structure with the MIL-53 topology and non-coordinated amino groups has been synthesized and characterized. Although catalytically active, strong adsorption and diffusion limitations make this amino-MOF unsuited for the studied reaction.

The behavior of the IRMOF-3 catalysts demonstrates that the basicity of the aniline-type amino group is enhanced when incorporated inside the IRMOF-3 structure. The catalysts are stable under the studied reaction conditions and could be reused without losing activity.

Acknowledgments

Senter Novem is gratefully acknowledged for financial support through the project EOSLT-04008 (Lange termijn EOS-onderzoeksprogramma). The X-ray facilities of the Department of Materials Science and Engineering of the Delft University of Technology is acknowledged for the XRD analyses. Prof. Em. dr. ir. H. van Bekkum is gratefully acknowledged for fruitful discussions.

References

[1] R.A. Sheldon, Pure Appl. Chem. 72 (2000) 1233–1246.
[2] J. Weitkamp, M. Hunger, U. Rymsa, Microporous Mesoporous Mater. 48 (2001) 255–270.
[3] F. Jerome, G. Kharchafi, I. Adam, J. Barrault, Green Chem. 6 (2004) 72–74.
[4] A. Corma, S. Iborra, I. Rodriguez, F. Sanchez, J. Catal. 211 (2002) 208–215.
[5] A. Corma, S.B.A. Hamid, S. Iborra, A. Velty, J. Catal. 234 (2005) 340–347.
[6] A. Corma, J. Catal. 216 (2003) 298–312.
[7] S. Kitagawa, R. Kitaura, S. Noro, Angew. Chem. Int. Ed. 43 (2004) 2334–2375.
[8] U. Mueller, M. Schubert, F. Teich, H. Puetter, K. Schierle-Arndt, J. Pastre, J. Mater. Chem. 16 (2006) 626–636.
[9] F.X. Llabrés i Xamena, O. Casanova, R. Galiasso Tailleur, H. Garcia, A. Corma, J. Catal. 255 (2008) 220–227.
[10] F.X. Llabres i Xamena, A. Abad, A. Corma, H. Garcia, J. Catal. 250 (2007) 294–298.
[11] S. Hasegawa, S. Horike, R. Matsuda, S. Furukawa, K. Mochizuki, Y. Kinoshita, S. Kitagawa, J. Am. Chem. Soc. 129 (2007) 2607–2614.
[12] Z.Q. Wang, S.M. Cohen, J. Am. Chem. Soc. 129 (2007) 12368.
[13] A.R. Millward, O.M. Yaghi, J. Am. Chem. Soc. 127 (2005) 17998–17999.
[14] J.S. Seo, D. Whang, H. Lee, S.I. Jun, J. Oh, Y.J. Jeon, K. Kim, Nature 404 (2000) 982–986.
[15] Y.K. Hwang, D.Y. Hong, J.S. Chang, S.H. Jhung, Y.K. Seo, J. Kim, A. Vimont, M. Daturi, C. Serre, G. Ferey, Angew. Chem. Int. Ed. 47 (2008) 4144–4148.
[16] O.M. Yaghi, M. O'Keeffe, N.W. Ockwig, H.K. Chae, M. Eddaoudi, J. Kim, Nature 423 (2003) 705–714.
[17] M. Eddaoudi, J. Kim, N. Rosi, D. Vodak, J. Wachter, M. O'Keeffe, O.M. Yaghi, Science 295 (2002) 469–472.
[18] M.J. Ingleson, J.P. Barrio, J.-B. Guilbaud, Y.Z. Khimyak, M.J. Rosseinsky, Chem. Commun. (2008) 2680–2682.
[19] D. Kim, T.B. Lee, S.B. Choi, J.H. Yoon, J. Kim, S.H. Choi, Chem. Phys. Lett. 420 (2006) 256–260.
[20] B. Arstad, H. Fjellvåg, K. Kongshaug, O. Swang, R. Blom, Adsorption 14 (2008) 755–762.
[21] T. Seki, M. Onaka, J. Mol. Catal. A Chem. 263 (2007) 115–120.
[22] S. Saravanamurugan, M. Palanichamy, M. Hartmann, V. Murugesan, Appl. Catal. A 298 (2006) 8–15.
[23] R. Wirz, D. Ferri, A. Baiker, Langmuir 22 (2006) 3698–3706.
[24] R.M. Martin-Aranda, E. Ortega-Cantero, M.L. Rojas-Cervantes, M.A. Vicente-Rodriguez, M.A. Banares-Munoz, J. Chem. Technol. Biotechnol. 80 (2005) 234–238.
[25] M.J. Climent, A. Corma, I. Dominguez, S. Iborra, M.J. Sabater, G. Sastre, J. Catal. 246 (2007) 136–146.
[26] I. Rodriguez, G. Sastre, A. Corma, S. Iborra, J. Catal. 183 (1999) 14–23.
[27] S.S. Kaye, A. Dailly, O.M. Yaghi, J.R. Long, J. Am. Chem. Soc. 129 (2007) 14176.
[28] M. Schubert, U. Müller, S. Marx, C. Kiener, J.R. Brown, G. Krennrich, International Patent WO/2008/052916, 2008.
[29] J.L.C. Rowsell, O.M. Yaghi, J. Am. Chem. Soc. 128 (2006) 1304–1315.
[30] T. Loiseau, C. Serre, C. Huguenard, G. Fink, F. Taulelle, M. Henry, T. Bataille, G. Ferey, Chem. Eur. J. 10 (2004) 1373–1382.
[31] S. Bauer, C. Serre, T. Devic, P. Horcajada, J. Marrot, G. Ferey, N. Stock, Inorg. Chem. 47 (2008) 7568–7576.
[32] C. Serre, F. Millange, C. Thouvenot, M. Nogues, G. Marsolier, D. Louer, G. Ferey, J. Am. Chem. Soc. 124 (2002) 13519–13526.
[33] A. Vimont, A. Travert, P. Bazin, J.C. Lavalley, M. Daturi, C. Serre, G. Ferey, S. Bourrelly, P.L. Llewellyn, Chem. Commun. (2007) 3291–3293.
[34] R. Srivastava, D. Srinivas, P. Ratnasamy, Microporous Mesoporous Mater. 90 (2006) 314–326.
[35] A.M. Ruppert, J.D. Meeldijk, B.W.M. Kuipers, B.H. Erne, B.M. Weckhuysen, Chem. Eur. J. 14 (2008) 2016–2024.

[36] B. Bonelli, B. Civalleri, B. Fubini, P. Ugliengo, C.O. Arean, E. Garrone, J. Phys. Chem. B 104 (2000) 10978–10988.
[37] S.G. Kazarian, M.F. Vincent, F.V. Bright, C.L. Liotta, C.A. Eckert, J. Am. Chem. Soc. 118 (1996) 1729–1736.
[38] C. Binet, M. Daturi, J.-C. Lavalley, Catal. Today 50 (1999) 207–225.
[39] J.L.C. Rowsell, O.M. Yaghi, Angew. Chem. Int. Ed. 44 (2005) 4670–4679.
[40] R.W. Alder, Chem. Rev. 89 (1989) 1215–1223.
[41] H.A. Staab, T. Saupe, Angew. Chem. Int. Ed. 27 (1988) 865–879.
[42] D.D. Das, P.J.E. Harlick, A. Sayari, Catal. Commun. 8 (2007) 829–833.
[43] S. Amirjalayer, M. Tafipolsky, R. Schmid, Angew. Chem. Int. Ed. 46 (2007) 463–466.
[44] X.F. Zhang, E.S.M. Lai, R. Martin-Aranda, K.L. Yeung, Appl. Catal. A 261 (2004) 109–118.
[45] M.L. Kantam, B.M. Choudary, C.V. Reddy, K.K. Rao, F. Figueras, Chem. Commun. (1998) 1033–1034.
[46] A. Massinon, J.A. Odriozola, P. Bastians, R. Conanec, R. Marchand, Y. Laurent, P. Grange, Appl. Catal. A 137 (1996) 9–23.
[47] L. Martins, R.T. Boldo, D. Cardoso, Microporous Mesoporous Mater. 98 (2007) 166–173.